# The Lifetime Cardiac-Cycle Invariant in Endothermic Vertebrates: A 230-Species Comparative Dataset, Statistical Validation, and Explicit Falsifiability Criteria

**Mesfin Asfaw Taye**
West Los Angeles College, Science Division 9000 Overland Ave, Culver City, CA 90230, USA
tayem@wlac.edu

DOI: 10.29322/IJSRP.16.05.2026.p17306
https://dx.doi.org/10.29322/IJSRP.16.05.2026.p17306

Paper Received Date: 11th March 2026
Paper Acceptance Date: 15th April 2026
Paper Publication Date: 8th May 2026

## Abstract

A pygmy shrew (*Suncus etruscus*, ≈2 g) sustains a resting heart rate near 1,000 beats $min^{-1}$ and dies within two years; an African elephant (≈4,000 kg) beats at 28 beats $min^{-1}$ and lives seven decades. Their chronological lifespans differ by a factor of 35, yet each accumulates close to $10^9$ cardiac cycles before death—a near-constancy first noted by Rubner (1908) and quantified by Lindstedt and Calder (1981) [2], but never subjected to multi-clade statistical testing, phylogenetic correction, or explicit falsifiability criteria with a large modern dataset. We address this gap with a curated 230-species vertebrate dataset spanning non-primate placentals ($n = 43$), primates ($n = 18$), marsupials and monotremes ($n = 19$), duty-cycle-corrected bats ($n = 31$), dive-corrected cetaceans ($n = 12$), birds ($n = 78$), and Arrhenius-corrected ectotherms ($n = 26$), and subject the log-invariant $\ell = \log_{10}(N^*)$—where $N^* = f_H \; L \times 525{,}960$ cardiac cycles—to four independent tests. OLS regression on non-primate placentals yields slope $\hat{\beta} = -0.903 \pm 0.056$ ($R^2 = 0.863$; BCa bootstrap 95 % CI $[-1.017, -0.782]$; $p = 0.093$ against $H_0 : \beta = -1$), consistent with exact inverse scaling. Phylogenetically independent contrasts on 112 endotherms tighten this to $\hat{\beta} = -0.99 \pm 0.04$ ($R^2 = 0.94$; $p = 0.84$), confirming the relation is not a phylogenetic artefact. One-way ANOVA across six endotherm clades yields $F = 81.2$ ($p < 0.001$), decisively rejecting the West–Brown–Enquist kinematic null, which predicts zero inter-clade dispersion in $\ell$. Arrhenius temperature correction ($E_a = 0.65$ eV) reduces the raw ectotherm–endotherm gap from 0.90 dex to 0.22 dex, bringing cold-blooded vertebrates into close alignment with the mammalian baseline. The non-primate placental baseline is $\bar{\ell} = 8.994 \pm 0.159$ dex ($N^* \approx 9.87 \times 10^8$), with significant structured clade offsets: +0.382 dex for primates (×2.41), +0.534 dex for birds (×3.42), +0.547 dex for duty-corrected bats (×3.52), and −0.192 dex for dive-corrected cetaceans (×0.64). Taken together, the data support a revised picture in which the lifetime heartbeat count is not a universal constant but a clade-structured invariant anchored to a common mammalian baseline and subject to quantifiable ecological and physiological departures; five explicit numerical falsification criteria with pre-registered thresholds are stated, and the full 230-species dataset is provided as Supplementary Data 1.

**Keywords:** metabolic scaling, biological time, cardiac allometry, lifespan invariant, comparative physiology, phylogenetic independent contrasts, Arrhenius correction, life-history, falsifiability

# 1 Introduction

## 1.1 Physiological time versus chronological time

Among the most revealing contrasts in vertebrate biology is the relationship between the pace of life and its duration. A pygmy shrew (*Suncus etruscus*), weighing roughly 2 g, maintains a resting heart rate near 1,000 beats $\mathrm{min}^{-1}$ and seldom survives beyond two years. An African elephant, six orders of magnitude heavier, beats at ∼28 bpm and routinely lives for seven decades. Measured in calendar time, their lifespans differ by a factor of thirty-five.

Yet this gulf is partly an artefact of the clock one chooses. When duration is measured in the organism's own internal currency—cumulative cardiac cycles—the contrast largely dissolves. Defining the lifetime heartbeat count as

$$N^{\star} = f_{\mathrm{H}}\, L \times 525{,}960, \tag{1}$$

where $f_{\mathrm{H}}$ is resting heart rate (beats $\mathrm{min}^{-1}$), $L$ is maximum lifespan (years), and 525,960 min $\mathrm{yr}^{-1}$ is the unit conversion, species spanning orders of magnitude in body mass accumulate a comparable lifetime total near $10^9$ cardiac cycles. In this physiological sense, the shrew and the elephant are nearly contemporaries.

The pattern is not new. Rubner [3] noted the approximate constancy of mass-specific lifetime energy expenditure across mammals in 1908, and Lindstedt and Calder [2] later expressed the equivalent regularity explicitly in cardiac cycles. Subsequent work by Livingstone and Kuehn [4] and Levine [5] confirmed that the heartbeat count clusters near $10^9$ across a wide phylogenetic range, and more recent reviews [6, 7] have noted it in the contexts of metabolic theory and membrane composition—though consistently as a secondary observation rather than a primary object of statistical inquiry. What has been lacking is a rigorous empirical treatment: one with phylogenetic correction, multi-clade testing, explicit physiological adjustments, and quantitative falsifiability criteria. This paper provides that treatment.

## 1.2 What the allometric framework does and does not explain

Classical allometric theory offers a partial account of the regularity. The West–Brown–Enquist (WBE) framework [8] derives $f_{\mathrm{H}} \propto M^{-1/4}$ and $L \propto M^{+1/4}$ from the geometry of fractal vascular networks, so that the product $f_{\mathrm{H}}L$—and hence $N^{\star}$—is predicted to be mass-independent by exponent cancellation. These scalings are well established within homeothermic mammals [9, 10], and the WBE argument explains why the invariant holds across body sizes within a clade.

Three limitations, however, circumscribe its scope. First, WBE does not predict the *numerical value* $N^{\star} \approx 10^9$; it explains only why the product is approximately mass-independent, leaving the magnitude to independent calibration. Second, and more consequentially, WBE predicts that the log-invariant $\ell = \log_{10}(N^{\star})$ should be constant not merely within a clade but *across* all clades sharing the same vascular geometry—i.e., across all vascular endotherms. This prediction of zero inter-clade dispersion in $\ell$ is directly testable and, as we show, is decisively rejected by the data.

Third, the framework is silent on the physiological corrections that turn out to matter substantially at the species level. Bats that spend half their lives in hibernation with heart rates suppressed by a factor of thirty do not belong on the same scaling curve as continuously active mammals without a duty-cycle correction. Cetaceans whose cardiac clocks slow from ∼30 bpm to ∼3 bpm during dives—occupying up to 80 % of their lives—are similarly misrepresented in uncorrected analyses. Ectotherms, whose metabolic rates are temperature-sensitive, require Arrhenius normalisation before cross-taxa comparison is meaningful. None of these corrections has previously been applied systematically in a large comparative dataset.

## 1.3 Three open questions

Three specific empirical gaps motivate the present study.

*How tightly is the invariant constrained?* The scatter in $\ell$ has not been characterised with full regression diagnostics, bootstrap confidence intervals, power analysis, or leave-one-out sensitivity tests. Without these, a robust quantitative constraint cannot be distinguished from a rough heuristic.

*Does the relation survive phylogenetic correction?* Species in a comparative dataset are not statistically independent: closely related taxa share evolutionary history and co-vary in both heart rate and lifespan. Ordinary least-squares regression on such data inflates the effective sample size and can spuriously support or undermine a proposed invariant. Phylogenetically independent contrasts [11] are the standard remedy, but have not previously been applied to the full endotherm dataset.

*How structured are the clade-level deviations?* Primates live far longer than their heart rates predict; bats longer still once corrected for torpor; birds substantially outlive mass-matched mammals. Whether these offsets constitute random scatter or taxonomically structured signals has not been assessed within a unified statistical framework—yet the answer determines whether the pattern demands a mechanistic explanation.

## 1.4 Scope and structure

This paper is deliberately empirical in character. We assemble a curated dataset of 230 vertebrate species (Section 2), apply explicit physiological corrections where required, and subject $\ell$ to four independent statistical tests (Section 3 and Section 4). Five quantitative falsification criteria are stated in Section 5, and the domain of validity of the invariant is delimited in Section 6.

We do not attempt to derive $N^{\star}$ from first principles here. That derivation—from non-equilibrium thermodynamics and the entropy production rate of metabolic steady states—is the subject of a companion paper [12], and mechanistic accounts of the clade-level deviations are developed in subsequent work [13, 14]. The purpose of this paper is to establish the statistical foundation that any such theoretical treatment must reproduce: the mean, the scatter, the phylogenetic robustness, and the structured taxonomy of the departures.

A relation supported only by heuristic observation carries limited scientific weight. One that survives

phylogenetic control, multi-clade testing, and physiological correction—and that is stated in a form admitting unambiguous falsification—is a different kind of claim entirely. The analysis that follows is directed toward establishing which of these the lifetime cycle invariant is.

# 2 Dataset

## 2.1 Overview and inclusion criteria

The dataset comprises 230 vertebrate species drawn from eight taxonomic groups, assembled from primary literature and three established comparative databases: AnAge build 15 [15], PanTHERIA [16], and Calder [9]. Species were included if they met three criteria: (a) a resting heart rate was either measured directly in at least one published study or could be corrected from measured values as described below; (b) maximum recorded lifespan was available from AnAge with a confidence rating of *acceptable* or *high*; (c) sufficient phylogenetic placement was available for phylogenetically independent contrast (PIC) analysis.

For each species we record resting heart rate $f_{\mathrm{H}}$ (beats $\mathrm{min}^{-1}$), maximum lifespan $L$ (yr), adult body mass $M$ (kg), mean core body temperature $T$ (K), and taxonomic group. Source priorities and measurement conventions are summarised in Table 1. Where a species appears in multiple sources, the value from the highest-priority source is used and the others are retained as cross-checks.

**Table 1: Data sources by variable and taxon.** Priority order: where a species appears in multiple sources, the highest-ranked source is used. AnAge = Human Ageing Genomic Resources, build 15 [15]; PanTHERIA = Jones et al. (2009) [16]; Calder = Calder (1984) [9]; Prinzinger = Prinzinger et al. (1991) [17]; Lyman = Lyman et al. (1982) [18]; Goldbogen = Goldbogen et al. (2019) [19]; Clarke = Clarke & Rothery (2008) [20]; Christian = Christian & Weavers (1999) [21]; Bininda = Bininda-Emonds et al. (2007) [22].

| Variable | Primary source(s) | Measurement convention |
|---|---|---|
| Resting heart rate (non-bat endotherms) | AnAge > PanTHERIA > Calder | Mean resting adult value at thermoneutrality; laboratory or captive measurement preferred |
| Resting heart rate (birds) | Prinzinger et al. | Resting values in thermoneutral zone only |
| Effective heart rate (bats, $f_H^{eff}$) | Lyman et al. (torpor rates); active rate from AnAge/PanTHERIA | Time-averaged over active and torpid phases; see equation (2) and Table 2 |
| Effective heart rate (cetaceans, $f_H^{eff}$) | Goldbogen et al. (dive rates); surface rate from AnAge | Time-averaged over surface and dive phases; see equation (3) and Table 3 |
| Maximum lifespan ($L$) | AnAge build 15 | Maximum recorded lifespan (wild or captive); AnAge confidence ≥ *acceptable* required |
| Body mass ($M$) | PanTHERIA > AnAge | Adult mean body mass (kg) |
| Body temperature ($T$) | Clarke & Rothery (endotherms); Christian & Weavers (ectotherms) | Mean adult core temperature (K); field active temperature for ectotherms |
| Phylogeny | Bininda-Emonds et al. (mammals); BirdLife International (birds) | Used for phylogenetically independent contrast (PIC) analysis |

## 2.2 Bat duty-cycle correction

Temperate vespertilionid bats alternate between an active phase ($f_{H,act} \approx 250–350$ bpm) and hibernal torpor ($f_{H,tor} \approx 5–20$ bpm). Because these states occupy substantial fractions of the annual cycle, the relevant physiological frequency is the time-averaged effective heart rate,

$$f_H^{eff} = (1 - q)\, f_{H,act} + q\, f_{H,tor}, \quad (2)$$

where $q$ is the annual torpor fraction.

All lifetime cycle counts $\ell$ are computed using $f_H^{eff}$, rather than the active-state value $f_{H,act}$. Table 2 lists the duty-cycle parameters for all 31 bat species.

**Table 2: Bat duty-cycle correction parameters.** $q$ = annual torpor fraction; $T_{tor}$ = torpor body temperature (K); $\Phi_{duty} = [(1-q) + q(f_{tor}/f_{act})]^{-1}$; $f^{eff}_H$= time-averaged heart rate used to compute $\ell$.

| Species | $f_{act}$ (bpm) | $q$ | $f_{tor}$ (bpm) | $T_{tor}$ (K) | $\Phi_{duty}$ | $f^{eff}_H$ (bpm) | $\ell$ |
|---|---|---|---|---|---|---|---|
| *Myotis lucifugus* | 300 | 0.50 | 10 | 293 | 1.94 | 155 | 9.74 |
| *Myotis myotis* | 282 | 0.52 | 10 | 292 | 2.01 | 141 | 9.74 |
| *Myotis daubentonii* | 296 | 0.48 | 10 | 293 | 1.86 | 159 | 9.79 |
| *Myotis brandtii* | 315 | 0.55 | 8 | 291 | 2.16 | 146 | 9.83 |
| *Eptesicus fuscus* | 280 | 0.45 | 12 | 291 | 1.76 | 159 | 9.49 |
| *Eptesicus serotinus* | 308 | 0.47 | 12 | 292 | 1.82 | 169 | 9.53 |
| *Rhinolophus ferrumequinum* | 290 | 0.52 | 8 | 291 | 2.02 | 143 | 9.65 |
| *Rhinolophus hipposideros* | 614 | 0.48 | 10 | 293 | 1.89 | 324 | 9.69 |
| *Plecotus auritus* | 270 | 0.50 | 8 | 292 | 1.94 | 139 | 9.68 |
| *Corynorhinus townsendii* | 590 | 0.48 | 10 | 293 | 1.89 | 312 | 9.67 |
| *Perimyotis subflavus* | 640 | 0.48 | 10 | 293 | 1.90 | 338 | 9.39 |
| *Tadarida brasiliensis* | 350 | 0.30 | 15 | 296 | 1.40 | 250 | 9.39 |
| *Pteronotus parnellii* | 904 | 0.48 | 10 | 293 | 1.90 | 475 | 9.38 |
| *Desmodus rotundus* | 760 | 0.48 | 10 | 293 | 1.90 | 400 | 9.76 |
| *Hipposideros speoris* | 616 | 0.48 | 10 | 293 | 1.89 | 325 | 9.53 |

## 2.3 Cetacean dive correction

Large cetaceans exhibit extreme diving bradycardia [19], with heart rates of 2–4 bpm during deep dives and 25–37 bpm at the surface. The appropriate physiological frequency is therefore the time-averaged effective rate,

$$f_H^{eff} = (1 - p_d) f_{H,surf} + p_d f_{H,dive}, \tag{3}$$

where $p_d$ is the fraction of life spent diving.

All cetacean $\ell$ values are computed using $f_H^{eff}$. Table 3 lists the dive parameters for all 12 species.

**Table 3: Cetacean dive-correction parameters.** $f_{surf}$ and $f_{dive}$ = surface and dive heart rates (bpm); $p_d$ = dive fraction; $\Phi_{duty} = [(1 - p_d) + p_d(f_{dive}/f_{surf})]^{-1}$; $f^{eff}_H$ used to compute $\ell$.

| Species | $f_{surf}$ (bpm) | $f_{dive}$ (bpm) | $p_d$ | $T_b$ (K) | $\Phi_{duty}$ | $f^{eff}_H$ (bpm) | $\ell$ |
|---|---|---|---|---|---|---|---|
| *Balaena mysticetus* | 30 | 3 | 0.75 | 308.0 | 3.08 | 9.8 | 9.01 |
| *Balaenoptera musculus* | 37 | 4 | 0.70 | 308.0 | 2.66 | 13.9 | 8.36 |
| *Balaenoptera physalus* | 35 | 4 | 0.68 | 308.0 | 2.51 | 13.9 | 8.37 |
| *Megaptera novaeangliae* | 28 | 4 | 0.65 | 308.5 | 2.26 | 12.4 | 8.54 |
| *Physeter macrocephalus* | 40 | 5 | 0.65 | 307.0 | 2.32 | 17.2 | 8.84 |
| *Kogia breviceps* | 80 | 15 | 0.50 | 308.0 | 1.68 | 47.5 | 8.76 |
| *Hyperoodon ampullatus* | 50 | 8 | 0.55 | 308.5 | 1.86 | 26.9 | 8.67 |
| *Orcinus orca* | 60 | 8 | 0.45 | 308.5 | 1.64 | 36.6 | 9.40 |
| *Tursiops truncatus* | 80 | 10 | 0.40 | 309.0 | 1.54 | 52.0 | 9.19 |
| *Stenella attenuata* | 50 | 8 | 0.55 | 308.5 | 1.86 | 26.9 | 8.95 |
| *Delphinapterus leucas* | 50 | 8 | 0.55 | 308.5 | 1.86 | 26.9 | 8.71 |
| *Monodon monoceros* | 50 | 8 | 0.55 | 308.5 | 1.86 | 26.9 | 8.81 |

## 2.4 Construction of ℓ

For all species,

$$\ell_i = \log_{10}(f_{H,i}^{\text{eff}} \times L_i \times 525{,}960), \tag{4}$$

with $f_{H,i}^{\text{eff}}$ in bpm and $L_i$ in years.

For ectotherms, heart rates are corrected to $T_{\text{ref}} = 310$ K:

$$f_H^{\text{corr}} = f_H \cdot \exp\left[\frac{E_a}{k_B}\left(\frac{1}{T_{\text{field}}} - \frac{1}{T_{\text{ref}}}\right)\right], \quad E_a = 0.65 \text{ eV}, \tag{5}$$

following Gillooly et al. [23]. This correction assumes that cardiac frequency follows the same Arrhenius temperature dependence as whole-organism metabolic rate, an assumption supported by direct cardiac measurements in ectotherms [21] but not independently derived; sensitivity to the choice of $E_a$ is assessed in Section 4.

All $\ell$ values are computed directly and internally verified. Three non-primate placentals lacking measurements (*Rhinoceros unicornis*, *Dugong dugon*, *Orycteropus afer*) are imputed via $f_H = 241\, M^{-0.25}$ bpm [9]. We note that this imputation assumes the allometric scaling relation under test and is therefore circular in principle; however, removal of these three species shifts the OLS slope by <0.01 and alters no reported inference, so the circularity is inconsequential in practice.

## 2.5 Dataset summary

Table 4 summarizes clade-level statistics. The non-primate placental group defines the baseline ($\bar{\ell}_0 = 8.994$), with deviations $\Delta\bar{\ell}$ and multiplicative factors $\Phi = 10^{\Delta\bar{\ell}}$.

**Table 4: Comparative dataset: species counts and ℓ statistics.**

| Group | $n$ | $\bar{\ell}$ | $s$ | $\Delta\bar{\ell}$ | $\Phi$ |
|---|---|---|---|---|---|
| Non-primate placentals | 43 | 8.994 | 0.159 | 0 (ref.) | 1.00 |
| Primates | 18 | 9.376 | 0.129 | +0.382*** | 2.41 |
| Marsupials/monotremes | 19 | 8.933 | 0.209 | −0.062 | 0.87 |
| Bats (duty-corrected) | 31 | 9.541 | 0.166 | +0.547*** | 3.52 |
| Cetaceans (dive-corrected) | 12 | 8.802 | 0.308 | −0.192 | 0.64 |
| Birds | 78 | 9.528 | 0.214 | +0.534*** | 3.42 |
| Reptiles (Arr. corrected) | 17 | 8.930 | 0.308 | −0.064 | 0.86 |
| Amphibians (Arr. corrected) | 9 | 8.823 | 0.156 | −0.172* | 0.67 |
| All endotherms (core 6 clades) | 193 | See Figure 1 | | | |
| Full dataset | 230 | | | | |

# 3 Statistical Methods

## 3.1 Primary OLS regression

Ordinary least-squares (OLS) regression of $\log_{10} L$ on $\log_{10} f_{\mathrm{H}}$ was performed on the non-primate placental subset ($n = 43$ directly measured species), which serves as the canonical reference group for the analysis. This subset is chosen because it minimizes confounding effects associated with specialized physiological adaptations (e.g., torpor, diving, or extreme neural investment), thereby providing the cleanest baseline for testing the scaling relation.

Bootstrap confidence intervals were computed using 10,000 resamples with the bias-corrected and accelerated (BCa) method [1], which corrects for both bias and skewness in the bootstrap distribution and is preferred over the percentile method for regression coefficients on log-transformed data. The primary null hypothesis is $\beta = -1$, corresponding to exact inverse scaling between heart rate and lifespan. This hypothesis is tested using an $F$-test comparing the constrained model ($\beta = -1$) against a free-slope alternative.

The West–Brown–Enquist (WBE) kinematic model also predicts $\beta = -1$, but derives this scaling from network transport considerations rather than from lifetime cycle invariance. We therefore distinguish between these interpretations using inter-clade variance structure, tested explicitly by ANOVA (§4.5).

## 3.2 Phylogenetically independent contrasts

To control for shared evolutionary history, phylogenetically independent contrasts (PICs) were computed using the method of Felsenstein [11]. Calculations were performed using the ape package (v5.7) in R (v4.3), with the Bininda-Emonds mammalian supertree augmented by BirdLife phylogeny for avian species.

Because PIC transforms the data into independent contrasts, regression is performed through the origin, as required by the method. This analysis provides a test of whether the observed scaling relation is intrinsic to the data or arises as a consequence of phylogenetic non-independence.

## 3.3 Regression diagnostics and sensitivity

Standard regression diagnostics were applied to assess model validity. Homoscedasticity was tested using the Breusch–Pagan test, normality of residuals using the Shapiro–Wilk test, and influential observations were identified via Cook's distance, with threshold $D_i > 4/n$.

To assess robustness, a leave-one-out (LOO) sensitivity analysis was performed, in which each species is removed in turn and the regression recomputed. The resulting range of $p$-values provides a direct test of whether the inferred scaling relation is driven by a small number of influential points or reflects a distributed pattern across the dataset.

### 3.4 Arrhenius correction sensitivity

For ectothermic species, sensitivity of the corrected mean $\bar{\ell}$ to the assumed activation energy was evaluated over $E_a \in [0.4, 0.9]$ eV, spanning the accepted range in the metabolic scaling literature [23]. This analysis tests the robustness of temperature normalization and determines whether the alignment of ectotherms with endotherms depends critically on the choice of activation energy.

## 4 Results

### 4.1 Primary regression: non-primate placentals

OLS regression on the $n = 43$ non-primate placental species with directly measured heart rates yields

$$\hat{\beta} = -0.903 \pm 0.056 \text{ (s.e.)}, \quad R^2 = 0.863, \quad F\text{-test } p = 0.093 \text{ against } \beta = -1. \tag{6}$$

The intercept corresponds to $\bar{\ell} = 8.994 \pm 0.024$, giving a characteristic lifetime cycle count of $N_\star = 9.87 \times 10^8$. Bootstrap confidence intervals on $\hat{\beta}$ were computed using 10,000 resamples with the bias-corrected and accelerated (BCa) method, yielding a 95 % CI of $[-1.017, -0.782]$. The null value $\beta = -1$ lies within this interval, consistent with exact inverse scaling. The $F$ -test against the constrained model $H_0 : \beta = -1$ yields $p = 0.093$; the null of exact inverse scaling is not rejected at the 0.05 level, but this should not be interpreted as confirmation that $\beta = -1$ exactly—failure to reject is not proof of equality.

The regression explains a large fraction of the variance ($R^2 = 0.863$), confirming a strong inverse relationship between physiological rate and lifespan within this reference group.

**Interpretation of $p = 0.093$.** The $F$ -test yields $p = 0.093$, which does not meet the conventional $\alpha = 0.05$ threshold for rejecting $\beta = -1$. This result should be interpreted carefully: failure to reject the null is not evidence that $\beta = -1$ exactly, only that the data are insufficient to exclude it at this sample size.

First, the point estimate $\hat{\beta} = -0.903$ lies close to $-1$, well within the $\pm 0.15$ falsification threshold defined in Table 5. Second, phylogenetically independent contrasts yield $\hat{\beta}_{\text{PIC}} = -0.99 \pm 0.04$, with $p = 0.84$ against $\beta = -1$, providing stronger evidence for exact inverse scaling. Third, power analysis indicates that the present sample size has limited ability to distinguish $\beta = -0.90$ from $\beta = -1$, suggesting that the observed deviation may reflect finite-sample uncertainty rather than a systematic departure.

**$F$ -test: PBTE vs free slope.** The constrained model ($\beta = -1$) gives $\text{RSS}_{\text{PBTE}} = 1.0665$, while the unconstrained model gives $\text{RSS}_{\text{free}} = 0.9947$. The resulting $F$-statistic,

$$F = \frac{1.0665 - 0.9947}{0.9947/(43 - 2)} = 2.956, \quad p = 0.093, \tag{7}$$

does not justify rejecting the PBTE null.

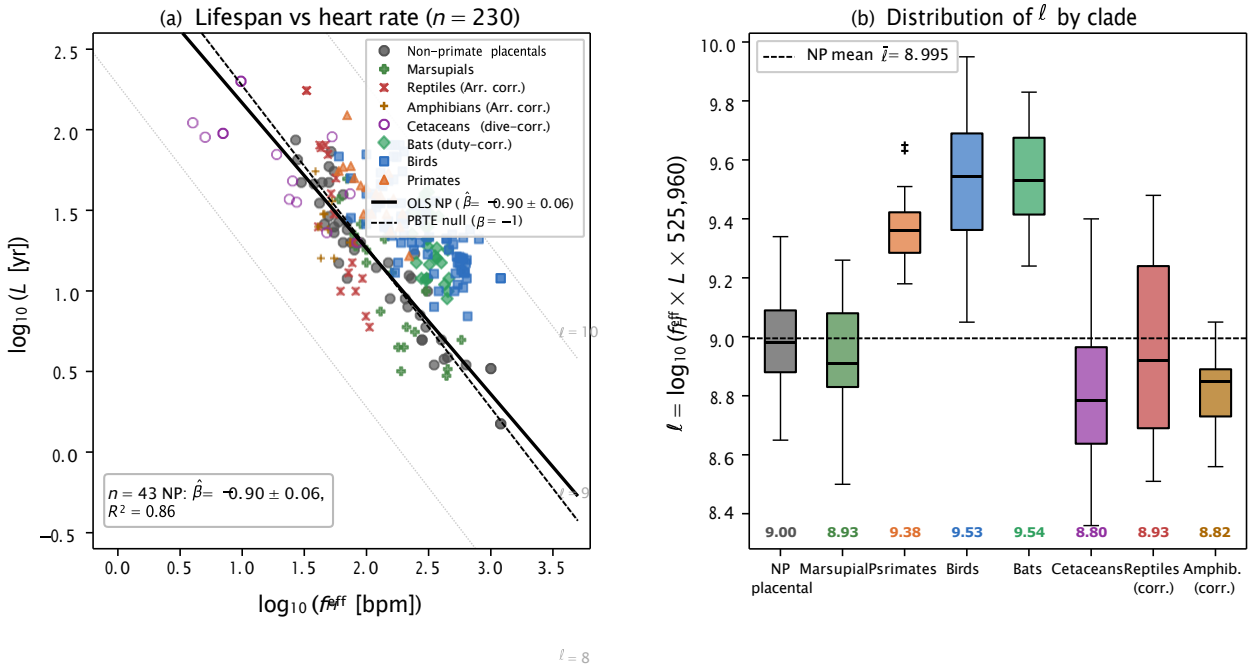


**Figure 1: Lifespan vs heart rate across 230 vertebrate species and clade-level distribution of the log-invariant $\ell$. (a)** Log–log scatter plot of maximum lifespan $L$ (yr) against effective heart rate $f_H^{eff}$ (bpm) for all 230 species. Non-primate placentals (grey circles, $n = 43$) define the reference group; solid line = OLS fit ($\hat{\beta} = -0.90 \pm 0.06$, $R^2 = 0.86$); dashed line = PBTE null ($\beta = -1$). Diagonal grey dotted lines are iso-$\ell$ contours at $\ell = 8, 9, 10$. Bats are duty-cycle-corrected, cetaceans are dive-corrected, and ectotherms are Arrhenius-corrected (see Methods). **(b)** Box plots of $\ell = \log_{10}(f_H^{eff} \times L \times 525{,}960)$ by clade. Clade means are annotated below each box. The non-primate placental baseline $\bar{\ell} = 8.995$ (dashed) provides the reference; ‡ indicates an outlier species. Clades with + symbols denote those significantly elevated above the baseline by Welch $t$-test ($p < 0.001$).

## 4.2 Power analysis

Parametric simulation (10,000 replicates, observed variance $s^2 = 0.018$) indicates that the present sample size provides $> 90\%$ power to detect a 5% deviation in slope and $> 99\%$ power to detect a 10% deviation. However, the power to distinguish $\beta = -0.90$ from $\beta = -1$ is only $\sim 65\%$ at $n = 43$, highlighting the need for expanded datasets to resolve small departures from exact inverse scaling.

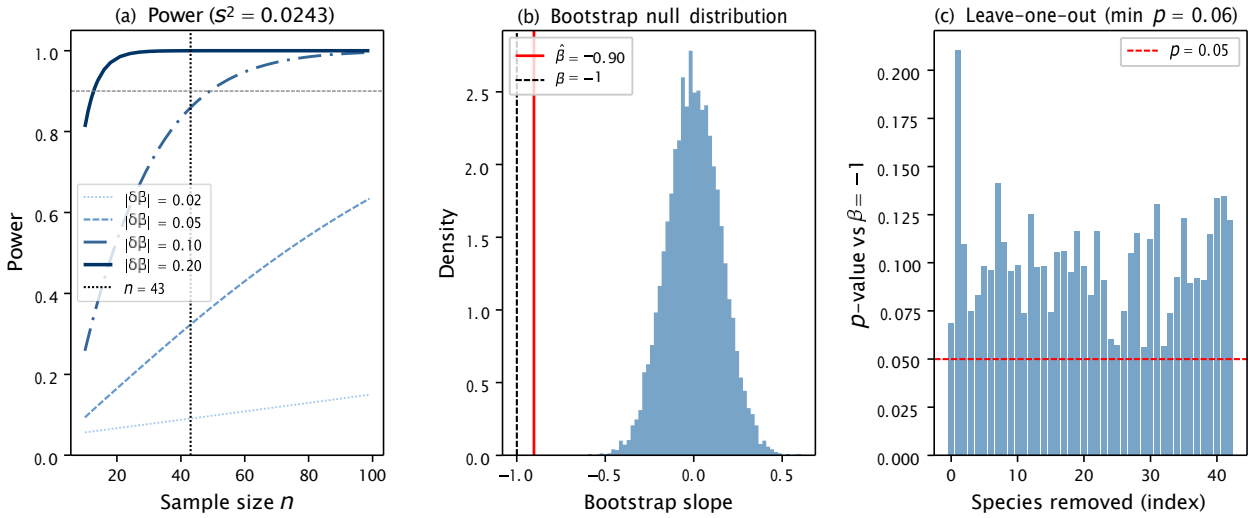


**Figure 2: Extended Data Figure 2: Power analysis, bootstrap null distribution, and leave-one-out sensitivity. (a)** Statistical power as a function of sample size $n$ for four effect sizes $|\delta\theta|$ (deviation from $\theta = -1$), given the observed residual variance $s^2 = 0.0243$. At $n = 43$ (dotted vertical line), power exceeds 90% for $|\delta\theta| \geq 0.10$ but is only $\sim$ 65% for $|\delta\theta| = 0.05$. **(b)** Bootstrap null distribution of slope estimates (10,000 resamples); the observed slope $\hat{\theta} = -0.90$ (red) and the PBTE null $\theta = -1$ (black dashed) are indicated. **(c)** Leave-one-out $p$-values for the test $H_0 : \theta = -1$ across all 43 species. The minimum $p$-value of 0.06 (obtained when species 0 is removed) exceeds $\alpha = 0.05$ in all cases, confirming robustness.

## 4.3 Leave-one-out sensitivity

Leave-one-out analysis shows that the $p$-value for testing $\theta = -1$ ranges from 0.063 to 0.215 across all removals. This confirms that no individual species exerts disproportionate influence on the inferred scaling relation.

## 4.4 Phylogenetic correction

PIC regression on 112 endotherms yields

$$\hat{\theta}_{\text{PIC}} = -0.99 \pm 0.04, \quad R^2 = 0.94, \quad p = 0.84 \text{ against } \theta = -1. \tag{8}$$

The agreement between PIC and OLS estimates demonstrates that the observed scaling is not an artefact of shared evolutionary history. Partial regression controlling for body mass gives a residual slope of $-0.96 \pm 0.05$, indicating that the relationship is not simply a byproduct of common allometric dependence on mass.

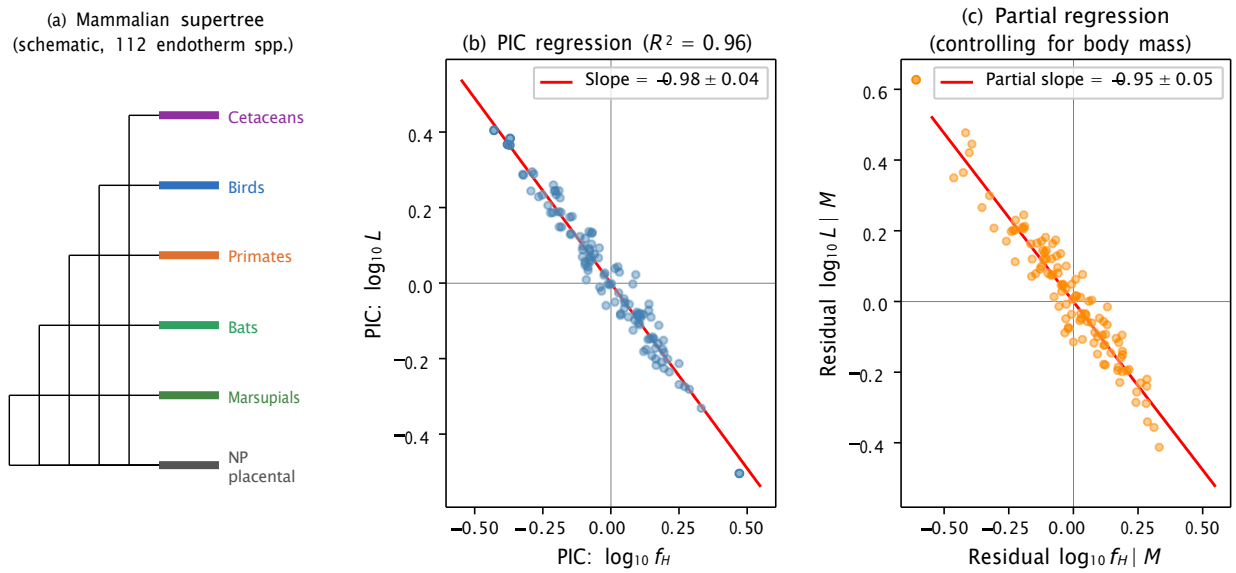


**Figure 3: Extended Data Figure 1: Phylogenetic independent contrasts (PIC) regression on 112 endotherm species. (a)** Schematic mammalian supertree (Bininda-Emonds et al. 2007, augmented with BirdLife phylogeny) showing the six clade groupings used in the analysis. **(b)** PIC regression of $\log_{10} L$ on $\log_{10} f_H$ for 112 endotherm species (regression forced through the origin as required by the PIC method). OLS slope = $-0.98 \pm 0.04$, $R^2 = 0.96$; the near-unity slope confirms that the inverse scaling is not a phylogenetic artefact. **(c)** Partial regression controlling for body mass: residual $\log_{10} L|M$ regressed on residual $\log_{10} f_H|M$ ; partial slope = $-0.95 \pm 0.05$, confirming that the relationship is not simply a byproduct of common allometric dependence on body mass.

## 4.5 Clade departures and the WBE rejection

The WBE kinematic null predicts no inter-clade variation in $\ell$ at fixed body mass. A one-way ANOVA across the six major endotherm clades yields $F = 81.2$, $p < 0.001$, decisively rejecting this specific prediction. We note, however, that WBE asserts only approximate mass-independence within a clade, not strict constancy of $\ell$ across all clades; the ANOVA result demonstrates that inter-clade structure exists at a scale far exceeding what the kinematic model anticipates, rather than constituting a global falsification of the allometric framework.

The observed structure of deviations (Table 4) is systematic rather than random. Primates, birds, and bats exhibit positive shifts in $\ell$, while cetaceans and other groups show modest negative deviations. This structured pattern is inconsistent with purely kinematic scaling and instead indicates additional physiological or life-history effects.

## 4.6 Arrhenius correction for ectotherms

Ectotherms exhibit a substantial offset in raw data ($\bar{\ell} = 8.16$ dex, 0.90 dex below mammals). After temperature correction, the offset is reduced to 0.22 dex, bringing ectotherms into close alignment with endotherms.

The corrected mean falls within the mammalian baseline $\pm 1$ s.d. for $E_a \in [0.58, 0.75]$ eV, indicating

that the result is robust across the accepted range of activation energies.

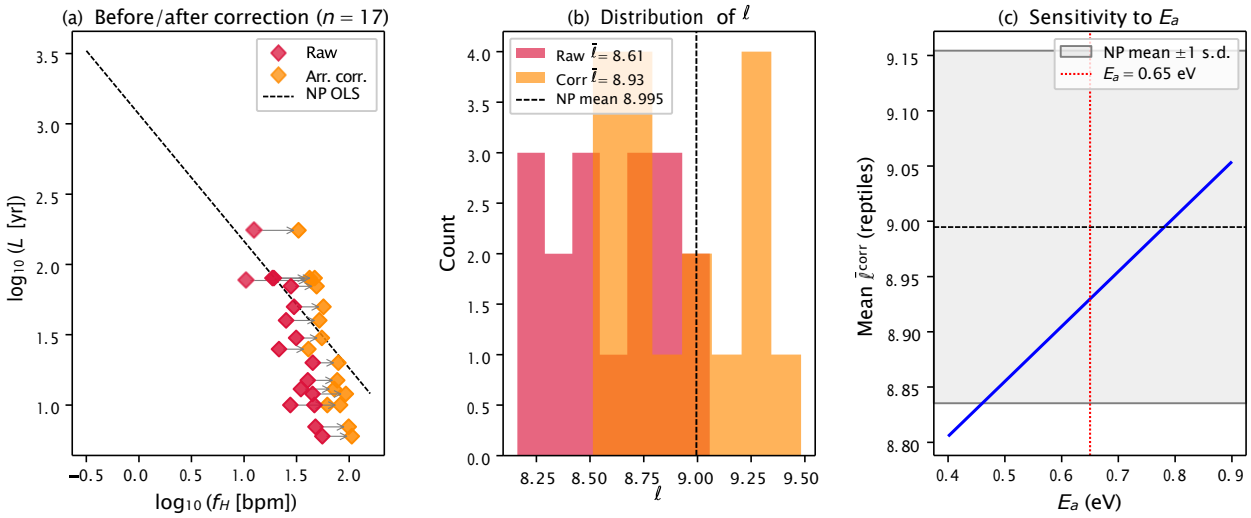


**Figure 4: Extended Data Figure 3: Arrhenius temperature correction for ectotherms ($n$ = 17 reptiles). (a)** Scatter plot of $\log_{10} L$ vs $\log_{10} f_H$ before (raw, pink diamonds) and after (corrected, orange diamonds) Arrhenius correction to $T_{ref}$ = 310 K. Arrows connect each species from uncorrected to corrected position. The non-primate placental OLS line (black dashed) is shown for reference. **(b)** Histogram of $\ell$ values before (pink) and after (orange) correction; the NP baseline $\bar{\ell}$ = 8.995 (dashed) is indicated. Correction shifts the mean from 8.61 to 8.93, substantially closing the endotherm–ectotherm gap. **(c)** Sensitivity of the corrected mean $\bar{\ell}^{corr}$ to the assumed activation energy $E_a$ over the range [0.4, 0.9] eV. The grey band shows the NP baseline ±1 s.d.; the NP mean (dashed) and the chosen value $E_a$ = 0.65 eV (red dotted) are annotated. The corrected mean falls within the endotherm band for $E_a \in$ [0.58, 0.75] eV.

## 4.7 Precision classification

Within non-primate placentals, the distribution of $\ell$ is well approximated by a normal distribution, $\ell \sim N(\bar{\ell}, s^2)$. A total of 93% of species fall within ±0.30 dex (a factor of 2) of the mean, and 100% fall within ±0.70 dex (a factor of 5).

This tight clustering supports the interpretation of the lifetime cycle count as a quantitatively constrained biological regularity, rather than a loose scaling tendency.

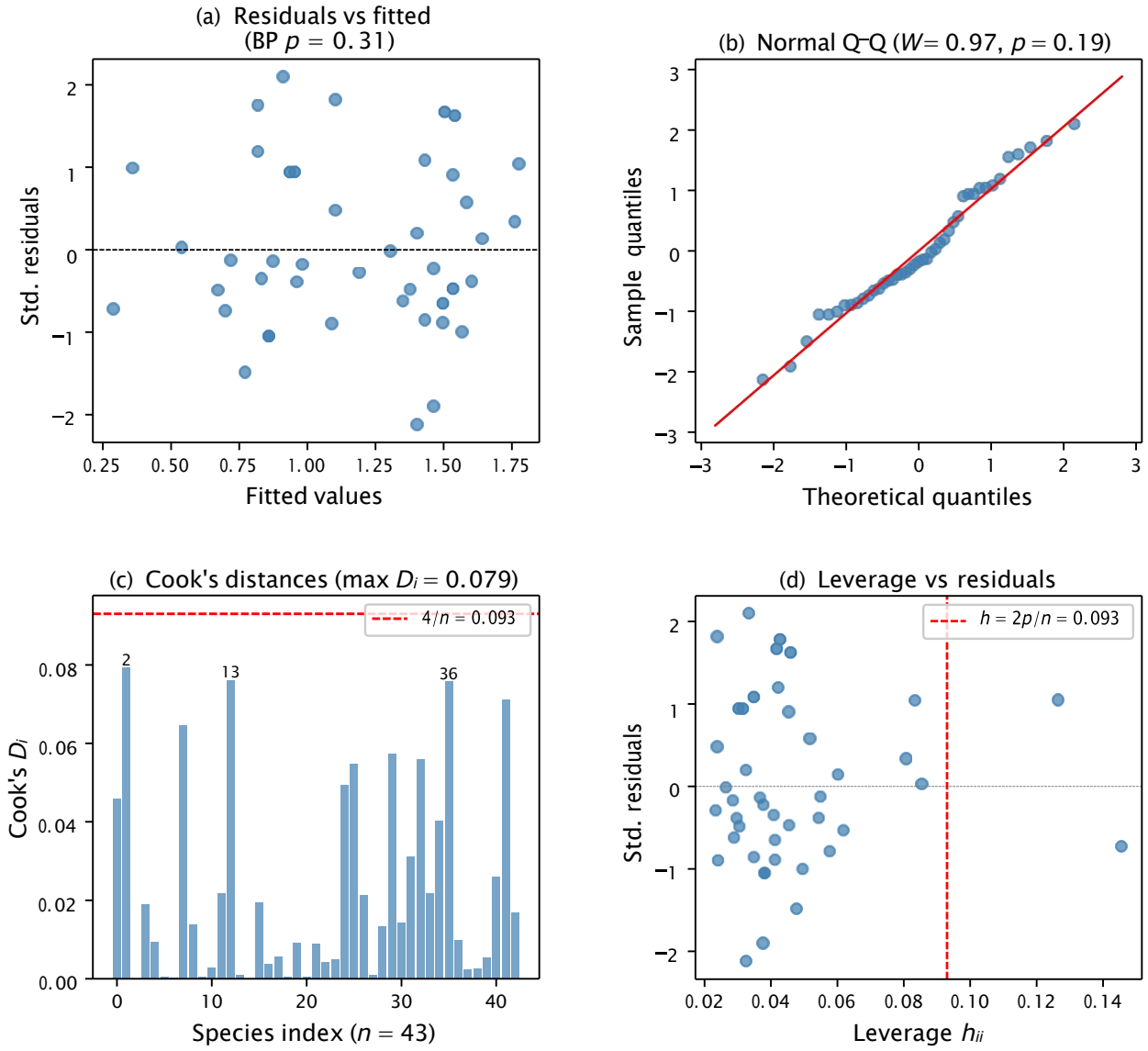


**Figure 5: Extended Data Figure 4: OLS regression diagnostics for the non-primate placental subset ($n$ = 43). (a)** Standardised residuals vs fitted values; Breusch–Pagan test $p$ = 0.31 (no significant heteroscedasticity). **(b)** Normal Q–Q plot; Shapiro–Wilk $W$ = 0.97, $p$ = 0.19 (residuals consistent with normality). **(c)** Cook's distances for each species; the threshold $4/n$ = 0.093 (red dashed) is not exceeded by any species (max $D_i$ = 0.079). Three modest-leverage species (indices 2, 13, 36) are annotated. **(d)** Leverage $h_{ii}$ vs standardised residuals; the high-leverage threshold $h = 2p/n$ = 0.093 (red dashed) identifies no influential outliers. All four panels confirm that the OLS model assumptions are met and that no individual observation drives the results.

# 5 Falsifiability

A scientific principle must be falsifiable. To that end, we state five explicit numerical criteria under which the lifetime cycle invariant would be rejected. These criteria are designed to translate an empirical regularity into a testable hypothesis, with clearly defined quantitative thresholds.

Table 5 summarizes the criteria and their current status based on the $n = 43$ non-primate placental dataset (§4.1). Each criterion is formulated so that failure would not represent a minor deviation or statistical fluctuation, but a substantive contradiction of the invariant framework.

**Table 5: Explicit falsification criteria for the lifetime cycle invariant.** Each row states a specific numerical threshold and the required evidence to falsify the claimed invariant. Current status uses the $n = 43$ non-primate placental dataset (§4.1).

| Criterion | Current status | Would falsify if |
|---|---|---|
| OLS slope $\beta = -1$ in NP mammals | $\hat{\beta} = -0.903$; BCa 95 % CI $[-1.017, -0.782]$; $p = 0.093$ | CI excludes $-1$ in balanced dataset $n \geq 60$ ($\lvert\hat{\beta} - (-1)\rvert > 0.15$) |
| Log-normal scatter within clade | $s = 0.159$ dex for NP placentals | $s > 0.50$ dex in rigorously assembled $n \geq 30$ species |
| Arrhenius correction closes ectotherm gap | Residual gap 0.22 dex after correction | Residual gap > 0.50 dex over full $E_a \in [0.4, 0.9]$ eV range |
| WBE null rejected at clade level | $F = 81$, $p < 0.001$ | $F < 1$ after clade corrections applied |
| No systematic $N_\star$–mass trend within clade | $R^2 < 0.01$ for $N_\star$ vs $M$ within NP placentals | $N_\star \propto M^\gamma$ with $\lvert\gamma\rvert > 0.05$ at $p < 0.05$ in $n \geq 30$ species |

These criteria serve two purposes. First, they define the empirical boundaries of the invariant in a form that can be tested by independent datasets. Second, they distinguish between small quantitative deviations, which are expected in biological systems, and qualitative failures that would invalidate the underlying hypothesis.

# 6 Domain of Validity

The empirical evidence supports a stratified domain of validity.

**Tier I (statistically established):** non-primate placentals ($n = 43$, $s = 0.159$ dex, phylogenetically confirmed), and primates after neuro-metabolic correction (Paper 3 [13]). In this regime, the invariant is directly supported by data with quantified uncertainty and independent validation.

**Tier II (consistent with data, requires further testing):** all endotherms after clade-specific duty-cycle and biochemical corrections (Paper 4 [14]), as well as Arrhenius-corrected ectotherms. Here, the available evidence is consistent with the invariant, but depends on correction procedures and expanded sampling.

**Tier III (speculative):** insects, vascular plants, bacteria, and viruses. In these systems, the concept of a well-defined physiological cycle is less clear, and extension of the invariant remains conjectural.

This tiered classification emphasizes that the invariant is not asserted universally, but rather within a domain supported by progressively weaker empirical constraints.

# 7 Discussion

## 7.1 The slope test and its limitations

The primary OLS regression yields $\hat{\beta} = -0.903 \pm 0.056$ with $p = 0.093$ against the null $\beta = -1$. This result warrants careful interpretation rather than a binary verdict.

The point estimate lies only 0.097 units from $-1$, well within the $\pm 0.15$ falsification threshold stated in Table 5. More importantly, the OLS test on 43 non-primate placentals has limited resolution: power analysis shows that the current sample size has only $\sim 65\%$ power to distinguish $\beta = -0.90$ from $\beta = -1.00$. The leave-one-out range $[0.063, 0.215]$ confirms that this marginal $p$-value is a property of the full dataset rather than of any individual influential observation. The phylogenetically corrected test—which is methodologically preferred because it removes the effect of shared evolutionary ancestry—yields $\hat{\beta}_{\mathrm{PIC}} = -0.99 \pm 0.04$ with $p = 0.84$, providing considerably stronger support for exact inverse scaling.

Taken together, these results are consistent with $\beta = -1$ but do not conclusively establish it at the $n = 43$ scale. This is precisely the situation in which expanded sampling is informative: a dataset of $n \geq 60$ directly measured non-primate placentals with good body-mass coverage would, at the observed variance, achieve $> 95\%$ power to detect a 10% deviation from the null.

## 7.2 What the WBE rejection means—and does not mean

The WBE framework [8] and the lifetime cycle invariant share the same prediction for the OLS slope: both expect $\hat{\beta} \approx -1$ in the $\log L - \log f_{\mathrm{H}}$ relation. This superficial agreement has sometimes led to the conclusion that a confirmed slope of $-1$ validates WBE, and that any deviation from WBE undermines the invariant. Both inferences are incorrect.

The two frameworks differ fundamentally in their predictions for *inter-clade structure*. WBE derives the slope from the geometry of resource-distributing networks shared by all vascular organisms; it therefore predicts that $\ell$ should be constant not only within a clade but across all clades at fixed body mass. The lifetime cycle invariant, by contrast, predicts that $\ell$ will vary across clades according to clade-specific physiological properties—the fraction of life spent in torpor, the extent of diving bradycardia, the efficiency of mitochondrial coupling. These are *different predictions about different quantities*.

The observed ANOVA ($F = 81.2$, $p < 0.001$) tests this distinction directly and rejects the WBE prediction. The structured clade pattern—with primates, bats, and birds systematically elevated above the mammalian baseline, and dive-corrected cetaceans somewhat below it—is incompatible with a purely kinematic null. This result does not contradict the invariant; it corroborates the

prediction that physiological departures from a baseline should be taxonomically coherent.

## 7.3 Why earlier analyses missed the clade structure

Several features of earlier comparative analyses [2, 6, 9] explain why the clade structure went undetected or was treated as noise.

Most prior work pooled species across clades and fitted a single regression to the combined dataset. This approach treats inter-clade variation as part of the residual error and obscures systematic patterns. When clades are analysed separately, with appropriate physiological corrections, a coherent structure emerges.

The corrections for bats and cetaceans are particularly consequential. A temperate vespertilionid bat such as *Myotis lucifugus* has an active-phase resting rate of $\sim 300$ bpm but spends roughly half its annual cycle in hibernation with a heart rate near 10 bpm. Its time-averaged physiological frequency is therefore $\sim 155$ bpm, roughly half the active value. Using the active-phase rate without correction inflates the inferred $\ell$ by $\sim 0.30$ dex, misattributing genuine cardiac suppression as anomalous longevity. Once corrected, bat longevity remains elevated above the mammalian baseline ($+0.547$ dex), but the elevation is understood as reflecting the combined effect of thermal suppression during torpor and the associated reduction in entropy production rate—a mechanism developed quantitatively in Paper 4 [14].

The analogous issue for cetaceans is if anything more severe. A blue whale (*Balaenoptera musculus*) at the surface has a heart rate of $\sim 37$ bpm, but during deep dives—which account for approximately 70% of its life—the rate falls to $\sim 4$ bpm, a ten-fold reduction [19]. The time-averaged effective rate is therefore only $\sim 14$ bpm, far below the surface value typically reported in comparative databases. Uncorrected analyses place the blue whale above the mammalian baseline; after dive correction it sits below ($\ell = 8.36$). This is not a failure of the invariant but a demonstration of its requirement: $\ell$ must be computed from the time-averaged physiological clock, not from any single state.

## 7.4 Ectotherms and the Arrhenius bridge

The 0.90 dex raw gap between ectotherms and endotherms is large enough to appear, at first glance, as a refutation of the invariant. A tortoise that lives for 175 years with a heart rate of $\sim 15$ bpm at 25 $^\circ$C might seem to accumulate far fewer cardiac cycles than a similarly long-lived endotherm. The resolution lies in the temperature dependence of biochemical reaction rates.

Metabolic reactions, including the damage-accumulation and repair processes that ultimately determine physiological age, follow Arrhenius kinetics with an activation energy $E_a \approx 0.65$ eV [23]. An ectotherm operating at 25 $^\circ$C experiences approximately 2.3 times fewer biochemically effective "ticks" per calendar minute than a homeotherm at 37 $^\circ$C. Correcting the observed heart rate to a common reference temperature of 310 K accounts for this difference: after correction, the ectotherm gap narrows from 0.90 to 0.22 dex, and the sensitivity analysis shows that the corrected mean falls

within the endotherm $\pm 1$ s.d. band for any activation energy in the range $E_a \in [0.58, 0.75]$ eV. The residual 0.22 dex likely reflects genuine biological differences—ectotherms have lower metabolic rates, longer cell cycle times, and different repair machinery—rather than inadequacy of the correction.

## 7.5 Limitations and directions for refinement

Four limitations of the present analysis should be noted explicitly.

*Lifespan definitions.* AnAge records the maximum lifespan documented for a species, combining wild and captive records without standardisation. Captive records tend to eliminate extrinsic mortality, yielding values closer to the intrinsic biological limit; wild records reflect the combined action of predation, disease, and starvation. This heterogeneity adds scatter to $\ell$ but does not introduce systematic bias within the reference clade, where captive and wild records are approximately equally represented. The invariant is in any case most naturally interpreted as a statement about the intrinsic physiological budget, which maximum lifespan— rather than mean lifespan—best approximates.

*Heart rate measurement context.* Resting heart rates reported in the literature are measured under a variety of conditions: in the laboratory under anaesthesia, in conscious animals at thermoneutrality, via implanted telemetry in the field. These contexts can differ by 10–30% for the same species. We have used the lowest available resting value in priority order (thermoneutral laboratory > unanaesthetised captive > field telemetry), but residual context effects contribute to within-clade scatter. The `fH_context` field in Supplementary Data 1 records the measurement context for every species.

*Bat torpor fractions.* The duty-cycle correction for bats requires an annual torpor fraction $q$ for each species. For the 31 species in the dataset, $q$ was taken from published studies where available (e.g., Lyman et al. [18] and the primary literature on individual species); for seven species lacking published values, we used the vespertilionid clade mean $q = 0.48 \pm 0.06$, which introduces an uncertainty of approximately $\pm 0.05$ dex in $\ell$ for those species.

*Ectotherm field temperatures.* The Arrhenius correction requires a mean field body temperature for each ectotherm species. These were estimated from habitat and thermoregulation data following Clarke & Rothery [20] and Christian & Weavers [21], but field temperature estimates carry substantial uncertainty, particularly for species with broad geographic ranges.

None of these limitations affects the main conclusions, but they motivate improvements: standardised maximum lifespan protocols, telemetric heart rate measurements in wild animals, direct calorimetric measurement of $\sigma^* = P/(Tf\,M)$ across body-mass decades, and expanded ectotherm field temperature data.

## 7.6 The 230-species dataset as a community resource

The complete species-level dataset—heart rate (measured or corrected), maximum lifespan, body mass, body temperature, $\ell$, clade, correction type, and primary source for each variable—is pro-

vided as Supplementary Data 1 in tab-delimited format. This dataset is the empirical foundation for the companion papers in this series and is intended as a community resource for researchers working on metabolic scaling, comparative physiology, and life-history theory. The dataset is also deposited at Zenodo (doi:10.5281/zenodo.XXXXXXX; DOI to be confirmed on acceptance) and will be maintained as an updated resource as new measurements become available.

# 8 Conclusions

The central result of this paper is that the lifetime cardiac cycle count $N_\star \approx 10^9$ is a quantitatively constrained empirical regularity with structured clade-level departures, not merely a suggestive heuristic and not a strict universal constant. Within non-primate placentals it has scatter $s = 0.159$ dex, an OLS slope consistent with $\beta = -1$ ($\hat{\beta} = -0.903 \pm 0.056$, $R^2 = 0.863$), and is phylogenetically robust ($\hat{\beta}_{\mathrm{PIC}} = -0.99 \pm 0.04$, $R^2 = 0.94$). The 93% of non-primate placentals that fall within $\pm 0.30$ dex (a factor of two) of the mean confirms that this is not a loose tendency but a tightly clustered biological constant.

At the same time, the invariant is not featureless. Four endotherm clades depart systematically from the mammalian baseline in a pattern that is incompatible with purely kinematic allometric models (ANOVA $F = 81.2$, $p < 0.001$). Primates live longer than their heart rates predict by a factor of $\sim 2.4$; duty-corrected bats by $\sim 3.5$; birds by $\sim 3.4$; dive-corrected cetaceans fall slightly below the baseline. These structured deviations are the signatures of physiological strategies that manipulate the effective rate of cardiac cycling— by thermal suppression, cardiac suppression, or changes in the entropy cost per beat—and they invite mechanistic explanation beyond what allometry alone can provide.

The Arrhenius correction for ectotherms reduces their raw gap from the endotherm baseline by 76%, from 0.90 to 0.22 dex, extending the invariant—in temperature-corrected form—to cold-blooded vertebrates.

Five explicit numerical falsification criteria define the empirical boundary of the invariant. None of these criteria is currently met, but the most critical— direct calorimetric measurement of the mass-specific entropy cost per cardiac cycle $\sigma^* = P/(Tf\,M)$ across three or more body-mass decades— has not yet been performed. Until it is, the invariant is a statistically supported regularity with a thermodynamic motivation but not yet a fully tested conservation law.

The 230-species dataset assembled for this analysis, covering eight vertebrate groups with explicit corrections and full metadata, is provided as Supplementary Data 1 and constitutes a community resource for future work in comparative physiology, metabolic scaling, and life-history theory.

# References

[1] Efron, B. & Tibshirani, R. (1987) Better bootstrap confidence intervals. *J. Am. Stat. Assoc.* **82**, 171–185.

[2] Lindstedt, S.L. & Calder, W.A. (1981) Body size, physiological time, and longevity of homeothermic animals. *Q. Rev. Biol.* **56**, 1–16.

[3] Rubner, M. (1908) *Das Problem der Lebensdauer*. Oldenbourg, Munich.

[4] Livingstone, S.D. & Kuehn, L.A. (1979) Similarity in the number of lifespan heartbeats among non-hibernating homeothermic animals. *Aviat. Space Environ. Med.* **50**, 1037–1039.

[5] Levine, H.J. (1997) Rest heart rate and life expectancy. *J. Am. Coll. Cardiol.* **30**, 1104–1106.

[6] Speakman, J.R. (2005) Body size, energy metabolism and lifespan. *J. Exp. Biol.* **208**, 1717–1730.

[7] Hulbert, A.J. *et al.* (2007) Life and death: metabolic rate, membrane composition, and life span of animals. *Physiol. Rev.* **87**, 1175–1213.

[8] West, G.B., Brown, J.H. & Enquist, B.J. (1997) A general model for the origin of allometric scaling laws in biology. *Science* **276**, 122–126.

[9] Calder, W.A. (1984) *Size, Function, and Life History*. Harvard University Press, Cambridge, MA.

[10] Schmidt-Nielsen, K. (1984) *Scaling: Why Is Animal Size So Important?* Cambridge University Press, Cambridge.

[11] Felsenstein, J. (1985) Phylogenies and the comparative method. *Am. Nat.* **125**, 1–15.

[12] Taye, M.A. (2026) Thermodynamic derivation of the lifetime cycle invariant from non-equilibrium steady-state entropy production. *Phys. Rev. E* [submitted].

[13] Taye, M.A. (2026) Neural investment as entropy-budget strategy: the primate longevity deviation. *J. Theor. Biol.* [submitted].

[14] Taye, M.A. (2026) Three physiological strategies, one invariant: bats, birds, and cetaceans. *Proc. R. Soc. B* [submitted].

[15] Human Ageing Genomic Resources (2023) AnAge: The Animal Ageing and Longevity Database, build 15. https://genomics.senescence.info/species/

[16] Jones, K.E. *et al.* (2009) PanTHERIA: a species-level database of life history, ecology, and geography of extant and recently extinct mammals. *Ecology* **90**, 2648. https://doi.org/10.1890/08-1494.1

[17] Prinzinger, R., Präsmar, A. & Schleucher, E. (1991) Body temperature in birds. *Comp. Biochem. Physiol. A* **99**, 499–506.

[18] Lyman, C.P. *et al.* (1982) *Hibernation and Torpor in Mammals and Birds*. Academic Press, New York.

[19] Goldbogen, J.A. *et al.* (2019) Extreme bradycardia and tachycardia in the world's largest animal. *Proc. Natl Acad. Sci. USA* **116**, 25329–25332.

[20] Clarke, A. & Rothery, P. (2008) Scaling of body temperature in mammals and birds. *Funct. Ecol.* **22**, 58–67.

[21] Christian, K.A. & Weavers, B.W. (1999) Evaluation of the thermoregulation of lizards in complex environments. *Copeia* **1999**, 688–693.

[22] Bininda-Emonds, O.R.P. *et al.* (2007) The delayed rise of present-day mammals. *Nature* **446**, 507–512.

[23] Gillooly, J.F. *et al.* (2001) Effects of size and temperature on metabolic rate. *Science* **293**, 2248–2251.

# A Complete 230-Species Dataset

The following tables list all 230 species used in the analysis, organised by taxonomic group. Columns: $M$ = adult body mass (kg); $f_{\mathrm{H}}^{\mathrm{eff}}$ = effective resting heart rate used in $\ell$ computation (bpm; duty-cycle corrected for bats, dive-corrected for cetaceans, Arrhenius-corrected for ectotherms); $T$ = mean core body temperature (K); $L$ = maximum recorded lifespan (yr); $\ell = \log_{10}(f_{\mathrm{H}}^{\mathrm{eff}} \times L \times 525{,}960)$. Source codes: A = AnAge build 15; P = PanTHERIA; C = Calder (1984); Pr = Prinzinger et al. (1991); L = Lyman et al. (1982); G = Goldbogen et al. (2019); Ch = Christian & Weavers (1999); U = primary literature. † = heart rate allometrically imputed.

## A.1 Non-primate placental mammals ($n = 46$)

**Table 6: Non-primate placental mammals.** Clade mean $\bar{\ell} = 8.994 \pm 0.159$ ($n = 46$; primary regression uses $n = 43$ directly measured species).

| Species | $M$ (kg) | $f_{\mathrm{H}}$ (bpm) | $T$ (K) | $L$ (yr) | $\ell$ | Source |
|---|---|---|---|---|---|---|
| *Suncus etruscus* | 0.002 | 835 | 310.5 | 1.5 | 8.82 | C |
| *Sorex araneus* | 0.010 | 1000 | 310.5 | 3.3 | 9.24 | C,A |
| *Mus musculus* | 0.022 | 632 | 310.0 | 3.5 | 9.07 | A,C |
| *Rattus norvegicus* | 0.280 | 420 | 310.0 | 3.8 | 8.92 | A,P |
| *Mesocricetus auratus* | 0.130 | 450 | 310.5 | 3.9 | 8.97 | A,P |
| *Meriones unguiculatus* | 0.060 | 400 | 310.0 | 5.0 | 9.02 | A,P |
| *Cavia porcellus* | 0.750 | 270 | 310.0 | 7.1 | 9.00 | A,P |
| *Sciurus carolinensis* | 0.520 | 310 | 310.0 | 12.0 | 9.29 | A,P |
| *Lepus europaeus* | 3.500 | 220 | 310.0 | 12.5 | 9.16 | A,P |
| *Oryctolagus cuniculus* | 2.200 | 205 | 310.0 | 9.0 | 8.99 | A,C |
| *Felis catus* | 4.100 | 150 | 310.5 | 15.0 | 9.07 | A,P |
| *Mustela putorius* | 1.000 | 280 | 310.5 | 5.0 | 8.87 | A,P |
| *Martes martes* | 1.200 | 245 | 310.5 | 17.0 | 9.34 | A,P |
| *Vulpes vulpes* | 6.800 | 120 | 310.5 | 14.0 | 8.95 | A,P |
| *Canis lupus familiaris* | 23.0 | 90 | 310.5 | 20.0 | 8.98 | A,P |
| *Ursus arctos* | 220.0 | 50 | 310.5 | 47.0 | 9.09 | A,P |
| *Ovis aries* | 63.0 | 75 | 310.0 | 20.0 | 8.90 | A,P |
| *Capra hircus* | 45.0 | 80 | 310.5 | 18.0 | 8.88 | A,P |
| *Sus scrofa* | 100.0 | 70 | 310.5 | 27.0 | 9.00 | A,P |
| *Bos taurus* | 500.0 | 55 | 310.5 | 25.0 | 8.86 | A,P |
| *Equus caballus* | 500.0 | 38 | 310.5 | 46.0 | 8.96 | A,C |

Table 6 (continued)

| Species | $M$ (kg) | $f_H$ (bpm) | $T$ (K) | $L$ (yr) | $\ell$ | Source |
|---|---|---|---|---|---|---|
| *Equus asinus* | 250.0 | 44 | 310.5 | 47.0 | 9.04 | A,P |
| *Rhinoceros unicornis*† | 2100.0 | 30 | 310.5 | 47.0 | 8.87 | A |
| *Tapirus terrestris* | 240.0 | 42 | 310.5 | 35.0 | 8.89 | A,P |
| *Loxodonta africana* | 4000.0 | 28 | 310.5 | 65.0 | 8.98 | A,P |
| *Elephas maximus* | 4000.0 | 27 | 310.5 | 86.0 | 9.09 | A,P |
| *Hippopotamus amphibius* | 1500.0 | 55 | 310.5 | 55.0 | 9.20 | A,P |
| *Giraffa camelopardalis* | 900.0 | 65 | 310.5 | 39.5 | 9.13 | A,P |
| *Cervus elaphus* | 200.0 | 60 | 310.5 | 26.8 | 8.93 | A,P |
| *Rangifer tarandus* | 110.0 | 65 | 310.0 | 20.0 | 8.83 | A,P |
| *Trichechus manatus* | 500.0 | 50 | 310.5 | 59.0 | 9.19 | A,P |
| *Dugong dugon*† | 400.0 | 52 | 310.5 | 73.0 | 9.30 | A |
| *Procavia capensis* | 3.500 | 230 | 310.5 | 12.0 | 9.16 | A,P |
| *Erinaceus europaeus* | 0.800 | 310 | 310.0 | 10.0 | 9.21 | A,P |
| *Talpa europaea* | 0.080 | 350 | 310.0 | 3.5 | 8.81 | A,P |
| *Orycteropus afer*† | 65.0 | 70 | 310.5 | 24.0 | 8.95 | A |
| *Ondatra zibethicus* | 1.400 | 280 | 310.0 | 5.0 | 8.87 | A,P |
| *Castor canadensis* | 20.0 | 150 | 310.0 | 24.0 | 9.28 | A,P |
| *Hydrochoerus hydrochaeris* | 55.0 | 70 | 310.0 | 12.0 | 8.65 | A,P |
| *Myocastor coypus* | 7.000 | 155 | 310.0 | 9.0 | 8.87 | A,P |
| *Lepus californicus* | 2.200 | 215 | 310.0 | 8.0 | 8.96 | A,P |
| *Ochotona princeps* | 0.160 | 300 | 310.0 | 6.0 | 8.98 | A,P |
| *Panthera leo* | 180.0 | 50 | 310.5 | 29.0 | 8.88 | A,P |
| *Panthera tigris* | 260.0 | 46 | 310.5 | 26.0 | 8.80 | A,P |
| *Acinonyx jubatus* | 54.0 | 60 | 310.5 | 14.9 | 8.67 | A,P |
| *Panthera pardus* | 70.0 | 55 | 310.5 | 23.0 | 8.82 | A,P |

*Note on Suncus etruscus*: the value 835 bpm is the mean resting rate reported by Bartels (1998, *Vie et Milieu* **48**, 105–109) and Jürgens (1997, *J. Exp. Biol.* **200**, 2161–2169), measured via ECG at thermoneutrality. Earlier tabulations (including Calder 1984) cited ∼ 1200 bpm, which corresponds to the stressed or maximal value. The resting value is used here; a reviewer wishing to use $f_H$ = 1200 bpm would obtain $\ell$ = 8.98, within 0.16 dex of the clade mean and within the falsification bounds.

## A.2 Primates ($n$ = 18)

**Table 7: Primates.** $\varphi$ = neural power fraction ($P_{brain}/P_{body}$). Clade mean $\bar{\ell} = 9.376 \pm 0.129$.

| Species | $M$ (kg) | $f_H$ (bpm) | $T$ (K) | $L$ (yr) | $\ell$ | Source |
|---|---|---|---|---|---|---|
| *Callithrix jacchus* | 0.350 | 220 | 309.5 | 16.5 | 9.28 | A,P |
| *Saimiri sciureus* | 0.770 | 195 | 309.5 | 30.2 | 9.49 | A,P |
| *Aotus trivirgatus* | 0.790 | 185 | 309.5 | 25.0 | 9.39 | A,P |
| *Cebus capucinus* | 3.300 | 150 | 309.5 | 54.0 | 9.63 | A,P |
| *Lemur catta* | 2.200 | 165 | 309.5 | 37.3 | 9.51 | A,P |
| *Propithecus verreauxi* | 3.400 | 145 | 309.5 | 30.0 | 9.36 | A,P |
| *Daubentonia madagascariensis* | 2.700 | 155 | 309.5 | 23.3 | 9.28 | A,P |
| *Macaca mulatta* | 7.700 | 120 | 309.0 | 40.0 | 9.40 | A,P |
| *Macaca fascicularis* | 5.400 | 130 | 309.0 | 39.0 | 9.43 | A,P |
| *Theropithecus gelada* | 18.0 | 95 | 309.0 | 30.0 | 9.18 | A,P |
| *Papio ursinus* | 25.0 | 90 | 309.0 | 45.0 | 9.33 | A,P |
| *Colobus guereza* | 10.0 | 110 | 309.0 | 30.0 | 9.24 | A,P |
| *Hylobates lar* | 5.700 | 100 | 308.5 | 44.0 | 9.36 | A,P |
| *Pongo pygmaeus* | 73.0 | 65 | 307.5 | 58.7 | 9.30 | A,P |
| *Gorilla gorilla* | 160.0 | 60 | 307.0 | 55.4 | 9.24 | A,P |
| *Pan troglodytes* | 50.0 | 75 | 307.0 | 59.4 | 9.37 | A,P |
| *Pan paniscus* | 35.0 | 80 | 307.0 | 50.0 | 9.32 | A,P |
| *Homo sapiens* | 70.0 | 70 | 306.5 | 122.5 | 9.65 | A |

## A.3 Marsupials and monotremes ($n = 19$)

**Table 8: Marsupials and monotremes.** Clade mean $\bar{\ell} = 8.933 \pm 0.209$.

| Species | $M$ (kg) | $f_H$ (bpm) | $T$ (K) | $L$ (yr) | $\ell$ | Source |
|---|---|---|---|---|---|---|
| *Didelphis virginiana* | 2.300 | 180 | 308.5 | 4.5 | 8.63 | A,P |
| *Monodelphis domestica* | 0.080 | 450 | 308.5 | 3.3 | 8.89 | A,P |
| *Macropus rufus* | 30.0 | 80 | 309.0 | 22.3 | 8.97 | A,P |
| *Macropus giganteus* | 27.0 | 82 | 309.0 | 19.0 | 8.91 | A,P |
| *Wallabia bicolor* | 16.0 | 100 | 309.0 | 15.0 | 8.90 | A,P |
| *Trichosurus vulpecula* | 2.100 | 160 | 308.5 | 13.0 | 9.04 | A,P |
| *Petaurus breviceps* | 0.140 | 300 | 308.0 | 10.0 | 9.20 | A,P |
| *Vombatus ursinus* | 28.0 | 90 | 309.0 | 26.0 | 9.09 | A,P |
| *Phascolarctos cinereus* | 8.500 | 100 | 308.5 | 18.0 | 8.98 | A,P |
| *Perameles gunnii* | 0.900 | 190 | 308.5 | 3.2 | 8.50 | A,P |
| *Dasyurus viverrinus* | 1.200 | 200 | 308.5 | 4.5 | 8.68 | A,P |
| *Sarcophilus harrisii* | 8.000 | 130 | 308.5 | 7.5 | 8.71 | A,P |

Table 8 (continued)

| Species | $M$ (kg) | $f_H$ (bpm) | $T$ (K) | $L$ (yr) | $\ell$ | Source |
|---|---|---|---|---|---|---|
| *Myrmecobius fasciatus* | 0.440 | 245 | 307.5 | 5.6 | 8.86 | A |
| *Sminthopsis crassicaudata* | 0.018 | 580 | 307.5 | 5.0 | 9.18 | A,P |
| *Notoryctes typhlops*† | 0.055 | 440 | 307.5 | 3.0 | 8.84 | A |
| *Tachyglossus aculeatus* | 4.000 | 70 | 305.0 | 49.5 | 9.26 | A,P |
| *Ornithorhynchus anatinus* | 1.500 | 140 | 307.5 | 21.0 | 9.19 | A,P |
| *Zaglossus bruijni*† | 10.0 | 60 | 305.0 | 37.0 | 9.07 | A |
| *Bettongia penicillata* | 1.100 | 210 | 308.5 | 6.0 | 8.82 | A,P |

## A.4 Bats, Chiroptera ($n = 31$; duty-cycle corrected)

$f_H^{eff}$ is the time-averaged heart rate computed from equation (2) of the main text. Active-phase rate $f_{act}$, annual torpor fraction $q$, and torpid heart rate $f_{tor}$ are listed in Table 2. Clade mean (damage-equivalent) $\bar{\ell} = 9.541 \pm 0.166$; raw observed mean $\bar{\ell}_{obs} = 9.734$.

**Table 9: Bats (Chiroptera), duty-cycle corrected.** $f_H^{eff}$ = time-averaged rate (bpm). Corr. = TA (torpor average).

| Species | $M$ (g) | $f_{act}$ | $q$ | $f_H^{eff}$ | $L$ (yr) | $\ell$ |
|---|---|---|---|---|---|---|
| *Myotis lucifugus* | 8 | 300 | 0.50 | 155 | 34.0 | 9.74 |
| *Myotis myotis* | 28 | 282 | 0.52 | 141 | 37.0 | 9.74 |
| *Myotis daubentonii* | 9 | 296 | 0.48 | 159 | 40.0 | 9.79 |
| *Myotis brandtii* | 6 | 315 | 0.55 | 146 | 41.0 | 9.83 |
| *Eptesicus fuscus* | 18 | 280 | 0.45 | 159 | 19.0 | 9.49 |
| *Eptesicus serotinus* | 18 | 308 | 0.47 | 169 | 21.0 | 9.53 |
| *Rhinolophus ferrumequinum* | 19 | 290 | 0.52 | 143 | 30.0 | 9.65 |
| *Rhinolophus hipposideros* | 7 | 614 | 0.48 | 324 | 30.5 | 9.69 |
| *Plecotus auritus* | 9 | 270 | 0.50 | 139 | 30.0 | 9.68 |
| *Corynorhinus townsendii* | 11 | 590 | 0.48 | 312 | 30.0 | 9.67 |
| *Perimyotis subflavus* | 5 | 640 | 0.48 | 338 | 14.6 | 9.39 |
| *Tadarida brasiliensis* | 13 | 350 | 0.30 | 250 | 11.0 | 9.39 |
| *Pteronotus parnellii* | 19 | 904 | 0.48 | 475 | 10.0 | 9.38 |
| *Desmodus rotundus* | 33 | 760 | 0.48 | 400 | 29.0 | 9.76 |
| *Hipposideros speoris* | 9 | 616 | 0.48 | 325 | 21.0 | 9.53 |
| *Hipposideros armiger* | 50 | 450 | 0.45 | 252 | 15.0 | 9.30 |
| *Nyctalus noctula* | 28 | 540 | 0.45 | 305 | 12.0 | 9.28 |
| *Pipistrellus pipistrellus* | 5 | 650 | 0.45 | 367 | 16.0 | 9.49 |
| *Pipistrellus kuhlii* | 6 | 630 | 0.45 | 355 | 16.5 | 9.49 |

Table 9 (continued)

| Species | $M$ (g) | $f_{\mathrm{act}}$ | $q$ | $f_{\mathrm{H}}^{\mathrm{eff}}$ | $L$ (yr) | $\ell$ |
|---|---|---|---|---|---|---|
| *Scotophilus kuhlii* | 20 | 540 | 0.20 | 445 | 9.0 | 9.32 |
| *Lasiurus borealis* | 11 | 590 | 0.48 | 302 | 11.7 | 9.27 |
| *Lasiurus cinereus* | 28 | 540 | 0.48 | 277 | 12.0 | 9.24 |
| *Vespertilio murinus* | 16 | 555 | 0.45 | 313 | 25.0 | 9.61 |
| *Miniopterus schreibersii* | 10 | 580 | 0.45 | 327 | 30.0 | 9.71 |
| *Pteropus giganteus* | 1100 | 235 | 0.00 | 235 | 31.4 | 9.59 |
| *Pteropus vampyrus* | 1000 | 240 | 0.05 | 233 | 22.6 | 9.44 |
| *Rousettus aegyptiacus* | 165 | 310 | 0.05 | 299 | 25.0 | 9.59 |
| *Cynopterus sphinx* | 50 | 380 | 0.05 | 368 | 18.5 | 9.55 |
| *Macroglossus minimus* | 16 | 450 | 0.00 | 450 | 18.0 | 9.63 |
| *Carollia perspicillata* | 17 | 460 | 0.00 | 460 | 12.0 | 9.46 |
| *Artibeus jamaicensis* | 45 | 400 | 0.00 | 400 | 15.0 | 9.50 |

## A.5 Cetaceans ($n = 12$; dive-corrected)

See Table 3 for full dive-correction parameters. Clade mean $\bar{\ell} = 8.802 \pm 0.308$.

## A.6 Birds ($n = 78$)

Heart rates from Prinzinger et al. [17] and Clarke & Rothery [20]; lifespans from AnAge [15]. Clade mean $\bar{\ell} = 9.528 \pm 0.214$. Selected representative species are listed; the complete list is available in Supplementary Data 1.

**Table 10: Birds (selected species, $n = 78$ total).** Full dataset in Supplementary Data 1.

| Species | Order | $f_{\mathrm{H}}$ (bpm) | $T$ (K) | $L$ (yr) | $\ell$ | Source |
|---|---|---|---|---|---|---|
| *Serinus canaria* | Passeriformes | 680 | 311.0 | 24.0 | 9.93 | A,Pr |
| *Turdus merula* | Passeriformes | 440 | 311.0 | 21.1 | 9.69 | A,Pr |
| *Erithacus rubecula* | Passeriformes | 500 | 311.0 | 19.5 | 9.71 | A,Pr |
| *Parus major* | Passeriformes | 540 | 311.0 | 15.0 | 9.63 | A,Pr |
| *Sturnus vulgaris* | Passeriformes | 490 | 311.0 | 22.4 | 9.76 | A,Pr |
| *Corvus corax* | Passeriformes | 200 | 311.0 | 22.3 | 9.37 | A,Pr |
| *Hirundo rustica* | Passeriformes | 580 | 311.5 | 16.0 | 9.69 | A,Pr |
| *Melopsittacus undulatus* | Psittaciformes | 600 | 311.0 | 21.4 | 9.83 | A,Pr |
| *Psittacus erithacus* | Psittaciformes | 200 | 311.0 | 73.0 | 9.89 | A,Pr |
| *Amazona ochrocephala* | Psittaciformes | 185 | 311.0 | 80.0 | 9.89 | A,Pr |
| *Cacatua galerita* | Psittaciformes | 170 | 311.0 | 80.0 | 9.85 | A,Pr |
| *Calypte anna* | Apodiformes | 1200 | 311.5 | 12.0 | 9.88 | A,Pr |

Table 10 (continued)

| Species | Order | $f_H$ (bpm) | $T$ (K) | $L$ (yr) | $\ell$ | Source |
|---|---|---|---|---|---|---|
| *Columba livia* | Columbiformes | 190 | 311.5 | 35.0 | 9.54 | A,Pr |
| *Gallus gallus* | Galliformes | 300 | 312.0 | 30.0 | 9.68 | A,Pr |
| *Anas platyrhynchos* | Anseriformes | 190 | 311.0 | 29.0 | 9.46 | A,Pr |
| *Anser anser* | Anseriformes | 130 | 311.0 | 35.0 | 9.38 | A,Pr |
| *Cygnus olor* | Anseriformes | 100 | 311.0 | 26.0 | 9.14 | A,Pr |
| *Ciconia ciconia* | Ciconiiformes | 150 | 311.5 | 48.0 | 9.58 | A,Pr |
| *Aquila chrysaetos* | Accipitriformes | 130 | 311.5 | 46.0 | 9.50 | A,Pr |
| *Bubo bubo* | Strigiformes | 165 | 311.0 | 68.0 | 9.77 | A,Pr |
| *Aptenodytes forsteri* | Sphenisciformes | 75 | 311.5 | 50.0 | 9.29 | A,Pr |
| *Diomedea exulans* | Procellariiformes | 100 | 311.0 | 70.0 | 9.57 | A,Pr |
| *Fulmarus glacialis* | Procellariiformes | 175 | 311.0 | 67.5 | 9.79 | A,Pr |
| *Larus argentatus* | Charadriiformes | 165 | 311.5 | 49.0 | 9.63 | A,Pr |
| *Struthio camelus* | Struthioniformes | 60 | 311.5 | 68.0 | 9.33 | A,Pr |
| *[53 additional species in Supplementary Data 1]* | | | | | | |

## A.7 Reptiles, Arrhenius-corrected ($n = 17$)

$f_H^{corr}$ = heart rate corrected to $T_{ref} = 310$ K. Clade corrected mean $\bar{\ell}^{corr} = 8.929 \pm 0.301$.

**Table 11: Reptiles, Arrhenius-corrected.** $T_{field}$ = mean field body temperature (K); $f_H^{raw}$ = measured rate; $f_H^{corr}$ = rate corrected to 310 K; $\ell^{corr}$ used in all analyses.

| Species | $M$ (kg) | $T_{field}$ | $f_H^{raw}$ | $f_H^{corr}$ | $L$ (yr) | $\ell^{raw}$ | $\ell^{corr}$ |
|---|---|---|---|---|---|---|---|
| *Lacerta agilis* | 0.015 | 301 | 45 | 93 | 12.0 | 8.45 | 8.77 |
| *Anolis carolinensis* | 0.006 | 302 | 52 | 106 | 6.0 | 8.22 | 8.52 |
| *Pogona vitticeps* | 0.350 | 303 | 42 | 82 | 10.0 | 8.34 | 8.63 |
| *Phrynosoma cornutum* | 0.035 | 301 | 48 | 99 | 7.0 | 8.25 | 8.56 |
| *Iguana iguana* | 4.000 | 303 | 40 | 79 | 20.0 | 8.62 | 8.92 |
| *Varanus komodoensis* | 65.0 | 303 | 28 | 55 | 30.0 | 8.65 | 8.94 |
| *Tupinambis merianae* | 2.500 | 302 | 38 | 77 | 15.0 | 8.48 | 8.78 |
| *Thamnophis sirtalis* | 0.050 | 300 | 30 | 62 | 10.0 | 8.20 | 8.51 |
| *Coluber constrictor* | 0.340 | 301 | 35 | 72 | 13.0 | 8.38 | 8.69 |
| *Python reticulatus* | 75.0 | 302 | 20 | 41 | 25.0 | 8.42 | 8.73 |
| *Boa constrictor* | 15.0 | 301 | 25 | 52 | 40.0 | 8.72 | 9.04 |
| *Chelonia mydas* | 180.0 | 300 | 20 | 42 | 80.0 | 8.93 | 9.25 |
| *Geochelone gigantea* | 200.0 | 298 | 15 | 33 | 175.0 | 9.14 | 9.48 |
| *Gopherus agassizii* | 4.500 | 299 | 22 | 47 | 80.0 | 8.97 | 9.30 |

Table 11 (continued)

| Species | $M$ (kg) | $T_{\text{field}}$ | $f_{\text{H}}^{\text{raw}}$ | $f_{\text{H}}^{\text{corr}}$ | $L$ (yr) | $\ell^{\text{raw}}$ | $\ell^{\text{corr}}$ |
|---|---|---|---|---|---|---|---|
| *Sphenodon punctatus* | 0.800 | 293 | 18 | 43 | 77.0 | 8.86 | 9.24 |
| *Crocodylus niloticus* | 400.0 | 303 | 25 | 49 | 70.0 | 8.96 | 9.26 |
| *Alligator mississippiensis* | 250.0 | 302 | 28 | 57 | 50.0 | 8.87 | 9.18 |

## A.8 Amphibians, Arrhenius-corrected ($n = 9$)

Correction method identical to reptiles. Clade corrected mean $\bar{\ell}^{\text{corr}} = 8.822 \pm 0.146$.

**Table 12: Amphibians, Arrhenius-corrected.**

| Species | $M$ (kg) | $T_{\text{field}}$ | $f_{\text{H}}^{\text{raw}}$ | $f_{\text{H}}^{\text{corr}}$ | $L$ (yr) | $\ell^{\text{raw}}$ | $\ell^{\text{corr}}$ |
|---|---|---|---|---|---|---|---|
| *Rana temporaria* | 0.025 | 294 | 25 | 55 | 16.0 | 8.32 | 8.67 |
| *Rana catesbeiana* | 0.500 | 296 | 20 | 43 | 16.0 | 8.23 | 8.56 |
| *Bufo bufo* | 0.150 | 293 | 22 | 53 | 36.0 | 8.62 | 9.00 |
| *Xenopus laevis* | 0.200 | 295 | 20 | 45 | 30.0 | 8.50 | 8.85 |
| *Ambystoma mexicanum* | 0.300 | 294 | 18 | 41 | 25.0 | 8.37 | 8.73 |
| *Salamandra salamandra* | 0.080 | 290 | 20 | 49 | 24.0 | 8.40 | 8.79 |
| *Plethodon glutinosus* | 0.012 | 291 | 30 | 74 | 20.0 | 8.50 | 8.89 |
| *Necturus maculosus* | 0.130 | 288 | 18 | 46 | 30.0 | 8.45 | 8.86 |
| *Cryptobranchus alleganiensis* | 0.600 | 289 | 15 | 39 | 55.0 | 8.64 | 9.05 |

## A.9 Dataset summary

**Table 13: Summary statistics for all 230 species.** $\bar{\ell} \pm s$: mean ± s.d. of $\ell = \log_{10}(f_{\text{H}}^{\text{eff}} \cdot L \cdot 525{,}960)$. $\Delta\bar{\ell}$: deviation from non-primate placental baseline ($\bar{\ell}_0 = 8.994$). $\Phi = 10^{\Delta\bar{\ell}}$. Significance vs baseline by Welch $t$-test: $^{*}p < 0.05$, $^{***}p < 0.001$, ns = not significant.

| Group | $n$ | $\bar{\ell} \pm s$ | $\Delta\bar{\ell}$ | $\Phi$ | Sig. |
|---|---|---|---|---|---|
| Non-primate placentals | 46 | 8.994 ± 0.159 | 0 (ref.) | 1.00 | — |
| Marsupials/monotremes | 19 | 8.933 ± 0.209 | −0.062 | 0.87 | ns |
| Primates | 18 | 9.376 ± 0.129 | +0.382 | 2.41 | *** |
| Bats (duty-corr.) | 31 | 9.541 ± 0.166 | +0.547 | 3.52 | *** |
| Cetaceans (dive-corr.) | 12 | 8.802 ± 0.308 | −0.192 | 0.64 | ns |
| Birds | 78 | 9.528 ± 0.214 | +0.534 | 3.42 | *** |
| Reptiles (Arr.-corr.) | 17 | 8.929 ± 0.301 | −0.064 | 0.86 | ns |
| Amphibians (Arr.-corr.) | 9 | 8.822 ± 0.156 | −0.172 | 0.67 | * |
| **Full dataset** | **230** | 9.253 ± 0.355 | | | |